

## Nitrofurans drugs beyond redox cycling: Evidence of Nitroreduction-independent cytotoxicity mechanism

C. Gallardo-Garrido<sup>a,d</sup>, Y. Cho<sup>a</sup>, J. Cortés-Ríos<sup>a</sup>, D. Vasquez<sup>b</sup>, C.D. Pessoa-Mahana<sup>a</sup>, R. Araya-Maturana<sup>c</sup>, H. Pessoa-Mahana<sup>d,\*</sup>, M. Faundez<sup>a,\*</sup>

<sup>a</sup> Laboratorio de Farmacología y Toxicología Molecular, Facultad de Química y de Farmacia, Pontificia Universidad Católica de Chile, Chile

<sup>b</sup> Laboratorio de Síntesis y Desarrollo de Fármacos, Facultad de Ciencias Químicas y Farmacéuticas, Universidad de Chile, Chile

<sup>c</sup> Instituto de Química y Recursos Naturales, Universidad de Talca, Talca, Chile

<sup>d</sup> Departamento de Química Orgánica y Físicoquímica, Facultad de Ciencias Químicas y Farmacéuticas, Universidad de Chile, Chile

### ARTICLE INFO

#### Keywords:

Nitrofurans  
Cytotoxicity  
Reactive Oxygen Species  
Nitroreduction  
Hydrazone

### ABSTRACT

Nitrofurans (5-nitro-2-hydrazonefuran as pharmacophore) are a group of widely used antimicrobial drugs but also associated to a variety of side effects. The molecular mechanisms that underlie the cytotoxic effects of nitrofurans are not yet clearly understood. One-electron reduction of 5-nitro group by host enzymes and ROS production *via* redox cycling have been attributed as mechanisms of cell toxicity. However, the current evidence suggests that nitrofurans ROS generation by itself is incapable to explain the whole toxic effects associated to nitrofurans consumption, proposing a nitro-reduction independent mechanism of toxicity.

In the present work, a series of nitrated and non-nitrated derivatives of nitrofurans were synthesized and evaluated *in vitro* for their cytotoxicity, ROS-producing capacity, effect on GSH-S-transferase and antibacterial activity.

Our studies showed that in human cells non-nitrated derivatives were less toxic than parental drugs but, unexpectedly preserved the ability to generate intracellular ROS in similar amounts to nitrofurans despite not entering into a redox cycle mechanism. In addition, some non-nitrated derivatives although being incapable to generate ROS exhibited the highest cell toxicity among all derivatives. Inhibition of cytosolic glutathione-S-transferase activity by some derivatives was also observed. Finally, only nitrofurans derivatives displayed antibacterial effect.

Results suggest that the combined 2-hydrazonefuran moiety, redox cycling of 5-nitrofurans, and inhibitory effects on antioxidant enzymes, would be finally responsible for the toxic effects of the studied nitrofurans on mammalian cells.

### 1. Introduction

Nitrofurans are a family of antibacterial and antiparasitic drugs containing a 5-nitro-2-hydrazonefuran framework bearing an azomethine moiety (Schwan and Ebetino, 2000). These drugs have been in clinical use since the 60's and up to date, mainly nitrofurantoin, nitrofurazone, furazolidone, nifuroxazide and nifurtimox remain in use. Their mechanism of action has been attributed to the dielectronic reduction of 5-nitro group by nitroreductases from microorganisms, generating the electrophilic intermediaries nitroso and hydroxylamine which in turn can bind to DNA and other biomolecules in microorganisms (Hall et al., 2011). This unique feature of nitrofurans allows them to maintain a low resistance profile in microorganisms due to the

high energetic cost related to the generation of nitrofurans-resistant mutants (Sandegren et al., 2008).

Despite their good clinical efficacy, treatment using nitrofurans has been associated to a variety of severe side effects such as hepatotoxicity, gastrointestinal disorders, agranulocytosis, pulmonary fibrosis and some reports of peripheral neuropathy, compromising the treatments compliances (Castro et al., 2006; Goemaere et al., 2008; Letelier et al., 2017). The mechanisms that generate the toxic effects are still unknown, nonetheless, reactive oxygen species (ROS) generation from the monoelectronic reductive metabolism of 5-nitro group has been attributed as the main responsible mechanism (Moreno et al., 1984). Host flavoenzymes, e.g. NADPH-cytochrome P450 reductase, are able to catalyze the one-electron reduction of 5-nitro group generating a

Abbreviations: NFZ, nitrofurazone; NHT, nitrofurantoin; NFX, nifuroxazide; MEP, maps of electrostatic potential; PGR, pyrogallol red

\* Corresponding authors.

E-mail addresses: [hpessoa@ciq.uchile.cl](mailto:hpessoa@ciq.uchile.cl) (H. Pessoa-Mahana), [mfaundez@uc.cl](mailto:mfaundez@uc.cl) (M. Faundez).

<https://doi.org/10.1016/j.taap.2020.115104>

Received 1 March 2020; Received in revised form 16 May 2020; Accepted 4 June 2020

Available online 10 June 2020

0041-008X/ © 2020 Elsevier Inc. All rights reserved.

nitroanion radical which, in the presence of molecular oxygen enters into a redox cycling mechanism which leads to restoration of the 5-nitro group with superoxide radical anion release and subsequent ROS and oxidative stress generation (Wang et al., 2008).

Several studies consider the reactivity of the 5-nitro group as the main cytotoxicity determining factor. Recently, it was shown that nitrofurantoin hepatic cytotoxicity is determined by electronic deficiency on the nitrogen atom of the nitro group, which determines its reduction capacity and reactivity towards GSH (Li et al., 2019). In the latter, nitrofurantoin-containing compounds showed higher capacity to deplete glutathione compared to nitrobenzene-containing compounds. These findings can be rationalized in terms of electronic resonance, where the nitrofurantoin ring shows a low pi-electronic donation capacity towards the nitro group, increasing in consequence its electrophilic character.

Despite all of the studies focused on nitroreduction-related cytotoxicity, evidence suggests that biological effects of nitrofurans are not completely related to oxidative stress. When several cell lines are exposed to nitrofurantoin, cell viability is affected in different extent and is not correlated to cytochrome P450 reductase activity nor ROS generation (Wang et al., 2008). In addition, cellular effects of nitrofurans not related to ROS generation have been described: inhibition of aldehyde hydrogenase (ALDH) enzymes by nitrofurans (Sarvi et al., 2018; Zhou et al., 2012), nifuroxazide inhibition of STAT3 (Yang et al., 2015), and nitrofurantoin inhibition of a bacterial isoform of glutathione-S-transferase (GST) enzyme (Perito et al., 1996). Moreover, previous reports demonstrated that nitrofurantoin toxicity in erythrocytes is mediated by inhibition of glutathione reductase (Dershwitz and Novak, 1982). However, non-nitrated derivatives of nitrofurantoin which lack of inhibitory capacity are equally effective in causing ATP and GSH depletion through a still unknown mechanism (Dershwitz and Novak, 1980). The evidence displayed above suggests that the toxicity of nitrofurans does not depend exclusively on the 5-nitro group. In addition, it is important to note that NADPH-cytochrome P450 reductase is expressed in most host cells where the nitro group undergoes one-electron reduction triggering ROS generation, therefore, studying non-nitrated derivatives is important in order to determinate the role of this structural component in cytotoxicity mechanisms.

Considering that antibacterial drugs resistance has become a mayor global obstacle in therapy, a more complete SAR understanding of known cytotoxic drugs becomes relevant information when proposing new prototypes bearing both, better toxicity profile and higher efficacy. As mentioned before, nitrofurans have a unique mechanism of action. The presence of the 5-nitro-2-hydrazonylfuran skeleton confers a unique scaffold with the hydrazine/hydrazide moiety connected to a highly electronic deactivated furan ring. We postulate that the electronic deficiency of 2-hydrazonylfuran portion contributes to toxic effects of nitrofurans that are not related to ROS generation by redox cycling.

The objective of the present study is to determine the contribution of the 2-hydrazonylfuran moiety of nitrofurantoin drug pharmacophore on cell toxicity. We focused on the synthesis and *in vitro* cytotoxic evaluation of a series of nitrofurazone, nitrofurantoin and nifuroxazide derivatives where the 5-nitro group has been replaced by bromine and chlorine atoms (−I electron-withdrawing effect), and methyl group (soft +I electron-donor effect), whilst preserving the integrity of the pharmacophore and modifying the electronic properties.

## 2. Materials and methods

### 2.1. Chemistry

#### 2.1.1. Reagents

All reagents were obtained from different suppliers and used without further purification. Semicarbazide, 4-hydroxybenzhydrazide, 5-bromo-2-furaldehyde and 5-nitro-2-furaldehyde were obtained from Aksci (USA). Phenylhydrazine, benzoic hydrazide, 1-aminohydantoin,

Furfural and 5-methyl-2-furaldehyde were purchased from Sigma-Aldrich.

#### 2.1.2. General chemistry

Nuclear magnetic resonance spectra were recorded on a Bruker AM-400 instrument using DMSO- $d_6$  solutions containing tetramethylsilane as internal standard. Chemical shifts are expressed in parts per million (ppm) downfield from TMS,  $J$  values are given in Hertz for solutions in DMSO- $d_6$ ; multiplicity are abbreviated as follows: s: singlet; d: doublet; t: triplet; m: multiplet; and dd: doublet of doublet. Infrared spectra were recorded in KBr discs on a Bruker Vector 22 spectrophotometer and wavenumbers are reported in  $\text{cm}^{-1}$ . Melting points were determined in a Stuart SMP10 Melting Point Instrument and are uncorrected. High resolution mass spectra were recorded on a DSA-TOF AxION 2 TOF MS (Perkin Elmer, Shelton, CT, USA), positive mode.

#### 2.1.3. Calculation of maps of electrostatic potential (MEP)

Geometry optimization and molecular electrostatic potential maps were computed using *ab initio* Hartree-Fock calculations with the 6-31G\* basis set. All calculations were performed using Spartan '08 (Wavefunction, Inc., Irvine, CA). Molecular electrostatic potential maps of the molecules were mapped on the 0.002 isodensity surface of each molecule. The surface was color-coded according to the electrostatic potential, with electron rich regions (negative potential) colored red and electron poor regions (positive potential) colored blue.

#### 2.1.4. Synthesis of compounds: general procedure

The reactions were carried out as previously reported with modifications (Leite et al., 2008). Hydrazine derivatives (1 mmol) were dissolved in distilled water (5 ml) containing glacial acetic acid (100  $\mu\text{l}$ ) as catalyzer. The mixture was sonicated for 5 min in an Ultrasonic Cleaner SB-3200 DTD (220 V, 100 W, 40 kHz). Afterwards, the corresponding aldehydes (1 mmol, or 1 mmol in 100  $\mu\text{l}$  of DMSO) were added dropwise to the mixture reactions and kept sonicated for 30 min at room temperature. Then, the products were filtered, washed twice with ice-cold water and dried overnight in a vacuum oven.

2-(Furan-2-ylmethylene)hydrazine-1-carboxamide (**1a**). Brown solid (94% yield).  $^1\text{H}$  NMR (400 MHz, DMSO- $d_6$ )  $\delta$  ppm: 10.25 (s, 1H, NH), 7.76 (s, 1H, H-6), 7.73 (d,  $J = 1.8$  Hz, 1H, H-3), 6.79 (d,  $J = 3.5$  Hz, 1H, H-5), 6.56 (dd,  $J = 3.5, 1.8$  Hz, 1H, H-4), 6.33 (s, 2H, NH<sub>2</sub>);  $^{13}\text{C}$  NMR (101 MHz, DMSO- $d_6$ )  $\delta$  156.6, 149.9, 144.0, 130.0, 112.0, 110.9. Ir  $\nu$  ( $\text{cm}^{-1}$ ): 3456 (N-H), 3287 (N-H), 1698 (C=O), 1519 (C=C), 1435 (C=N). M.p. 203–208 °C. HRMS [ $\text{M}^+$ ]:  $\text{C}_6\text{H}_7\text{N}_3\text{O}_2$  calc 153.1390. Found 153.1382.

2-((5-Methylfuran-2-yl)methylene)hydrazine-1-carboxamide (**1b**). White solid (90% yield).  $^1\text{H}$  NMR (400 MHz, DMSO- $d_6$ )  $\delta$  ppm 10.16 (s, 1H, NH), 7.68 (s, 1H, H-6), 6.65 (d,  $J = 3.2$  Hz, 1H, H-3), 6.28 (s, 2H, NH<sub>2</sub>), 6.18 (d,  $J = 3.2$  Hz, 1H, H-4), 2.29 (s, 3H, CH<sub>3</sub>).  $^{13}\text{C}$  NMR (101 MHz, DMSO- $d_6$ )  $\delta$  157.0, 153.8, 148.7, 130.7, 113.1, 108.7, 13.9. Ir  $\nu$  ( $\text{cm}^{-1}$ ): 3456 (N-H), 3220 (N-H), 1674 (C=O), 1573 (N-H), 1442 (C=N). M.p. 200–204 °C. HRMS [ $\text{M}^+$ ]:  $\text{C}_7\text{H}_9\text{N}_3\text{O}_2$  calc 167.1656. Found 167.1666.

2-((5-Bromofuran-2-yl)methylene)hydrazine-1-carboxamide (**1c**). White solid (59% yield).  $^1\text{H}$  NMR (400 MHz, DMSO- $d_6$ )  $\delta$  ppm 10.29 (s, 1H, NH), 7.68 (s, 1H, H-6), 6.84 (d,  $J = 3.4$  Hz, 1H, H-3), 6.68 (d,  $J = 3.5$  Hz, 1H, H-4), 6.34 (s, 2H, NH<sub>2</sub>).  $^{13}\text{C}$  NMR (101 MHz, DMSO- $d_6$ )  $\delta$  ppm 156.3, 151.9, 128.8, 122.9, 114.0, 113.4. Ir  $\nu$  ( $\text{cm}^{-1}$ ): 3464 (N-H), 3325 (N-H), 1681 (C=O), 1573 (N-H), 1442 (C=N). M.p. dec. 210 °C. HRMS [ $\text{M}^+$ ]:  $\text{C}_6\text{H}_6\text{BrN}_3\text{O}_2$  calc 232.0346. Found 232.0350.

2-((5-Chlorofuran-2-yl)methylene)hydrazine-1-carboxamide (**1d**). White solid (80% yield).  $^1\text{H}$  NMR (400 MHz, DMSO- $d_6$ )  $\delta$  10.31 (s, 1H, NH), 7.69 (d, 1H, H-6), 6.88 (d,  $J = 3.5$  Hz, 1H, H-3), 6.60 (d,  $J = 3.5$  Hz, 1H, H-4), 6.35 (s, 2H, NH<sub>2</sub>).  $^{13}\text{C}$  NMR (101 MHz, DMSO- $d_6$ )  $\delta$  156.81, 150.21, 136.42, 129.25, 113.61, 109.64. Ir  $\nu$  ( $\text{cm}^{-1}$ ):

3456 (N-H), 3278 (N-H), 1705 (C=O), 1589 (N-H), 1427 (C=N). M.p. 186–188 °C. HRMS [ $M^+$ ]:  $C_6H_6ClN_3O_2$ ; calc 188.0227. Found 188.0229.

2-((5-Nitrofur-2-yl)methylene)hydrazine-1-carboxamide (nitrofurazone) (**1d**, **NFZ**). Yellow solid (97% yield).  $^1H$  NMR (400 MHz, DMSO- $d_6$ )  $\delta$  ppm 10.78 (s, 1H, NH), 7.79 (s, 1H, H-6), 7.76 (d,  $J = 4.0$  Hz, 1H, H-3), 7.22 (d,  $J = 4.0$  Hz, 1H, H-4), 6.61 (s, 2H, NH $_2$ ).  $^{13}C$  NMR (101 MHz, DMSO- $d_6$ )  $\delta$  156.4, 153.6, 151.7, 127.9, 115.7, 112.6. Ir  $\nu$  ( $cm^{-1}$ ): 3464–3294 (N-H), 1720 (C=O), 1581 (C=N), 1512 (NO $_2$ ), 1388 (NO $_2$ ). HRMS [ $M^+$ ]:  $C_6H_6N_4O_4$  calc 198.1366. Found 198.1366.

1-(Furan-2-ylmethylene)-2-phenylhydrazine (**2a**). Brown solid (97% yield).  $^1H$  NMR (400 MHz, DMSO- $d_6$ )  $\delta$  ppm 10.31 (s, 1H, NH), 7.79 (s, 1H, H-6), 7.70 (d,  $J = 1.8$  Hz, 1H, H-5), 7.22 (t,  $J = 7.7$  Hz, 2H, H-11), 7.02 (d,  $J = 7.7$  Hz, 2H, H-10), 6.75 (t,  $J = 7.7$  Hz, 1H, H-12), 6.64 (d,  $J = 3.4$  Hz, 1H, H-3), 6.55 (dd,  $J = 3.4, 1.8$  Hz, 1H, H-4).  $^{13}C$  NMR (101 MHz, DMSO- $d_6$ )  $\delta$  151.3, 145.5, 143.5, 129.6, 127.7, 119.3, 112.4, 112.3, 109.3, 60.2. Ir  $\nu$  ( $cm^{-1}$ ): 3317 (N-H), 1481 (C=N), 1512 (C=C), 1442 (C=C). M.p. dec. 86 °C. HRMS [ $M^+$ ]:  $C_{11}H_{10}N_2O$  calc 186.2104. Found 186.2106.

1-(5-Bromofuran-2-ylmethylene)-2-phenylhydrazine (**2b**). Brown solid (50% yield).  $^1H$  NMR (400 MHz, DMSO- $d_6$ )  $\delta$  ppm 10.39 (s, 1H, NH), 7.68 (s, 1H, H-6), 7.21 (t, 2H, H-11), 7.00 (d,  $J = 7.9$  Hz, 2H, H-10), 6.76 (t,  $J = 7.2$  Hz, 1H, H-12), 6.67 (d,  $J = 3.5$  Hz, 1H, H-3), 6.66 (d,  $J = 3.4$  Hz, 1H, H-4).  $^{13}C$  NMR (101 MHz, DMSO- $d_6$ )  $\delta$  ppm 152.9, 144.8, 129.1, 126.0, 121.7, 119.1, 113.8, 112.0, 111.2. Ir  $\nu$  ( $cm^{-1}$ ): 3302 (N-H), 1442 (C=N). M.p. > 300 °C. HRMS [ $M^+$ ]:  $C_{11}H_9BrN_2O$  calc 265.1060. Found 265.1066.

1-(5-Nitrofur-2-ylmethylene)-2-phenylhydrazine (**2c**). Red needles (98% yield).  $^1H$  NMR (400 MHz, DMSO- $d_6$ )  $\delta$  ppm 11.12 (s, 1H, NH), 7.78 (s, 1H, H-6), 7.73 (d,  $J = 4.0$  Hz, 1H, H-4), 7.27 (t,  $J = 7.7$  Hz, 2H, H-11), 7.12 (t,  $J = 7.7$  Hz, 2H, H-10), 6.98 (d,  $J = 4.0$  Hz, 1H, H-3), 6.86 (t,  $J = 7.7$  Hz, 1H, H-12).  $^{13}C$  NMR (101 MHz, DMSO- $d_6$ )  $\delta$  156.0, 151.4, 144.2, 129.7, 124.4, 121.0, 116.3, 113.3, 111.2. Ir  $\nu$  ( $cm^{-1}$ ): 3302 (N-H), 1597 (C=N), 1566 (NO $_2$ ), 1365 (NO $_2$ ), 1465 (C=C). M.p. 190–192 °C. HRMS [ $M^+$ ]:  $C_{11}H_9N_3O_3$  calc 231.2080. Found 231.2088.

1-((Furan-2-ylmethylene)amino)imidazolidine-2,4-dione (**3a**). White solid (90% yield).  $^1H$  NMR (400 MHz, DMSO- $d_6$ )  $\delta$  ppm 11.23 (s, 1H, NH), 7.81 (d,  $J = 1.8$  Hz, 1H, H-5), 7.69 (s, 1H, H-6), 6.83 (d,  $J = 3.4$  Hz, 1H, H-3), 6.62 (dd,  $J = 3.4, 1.8$  Hz, 1H, H-4), 4.32 (s, 2H, CH $_2$ ).  $^{13}C$  NMR (101 MHz, DMSO- $d_6$ )  $\delta$  169.0, 153.4, 149.5, 144.9, 133.3, 113.0, 112.2, 48.9. Ir  $\nu$  ( $cm^{-1}$ ): 1782 (C=O), 1720 (C=O), 1481 (C=N), 1442 (CH $_2$ ). M.p. dec. 220 °C. HRMS [ $M^+$ ]:  $C_8H_7N_3O_3$  calc 194.0560. Found 194.1872

1-((5-Methylfuran-2-ylmethylene)amino)imidazolidine-2,4-dione (**3b**). White solid (88% yield).  $^1H$  NMR (400 MHz, DMSO- $d_6$ )  $\delta$  ppm 11.20 (s, 1H, NH), 7.61 (s, 1H, H-6), 6.70 (d,  $J = 3.3$  Hz, 1H, H-3), 6.23 (d,  $J = 3.3$  Hz, 1H, H-4), 4.30 (s, 2H, CH $_2$ ), 2.33 (s, 3H, CH $_3$ );  $^{13}C$  NMR (101 MHz, DMSO- $d_6$ )  $\delta$  169.4, 154.5, 153.7, 148.4, 133.7, 115.2, 108.9, 49.3, 13.9. Ir  $\nu$  ( $cm^{-1}$ ): 11782 (C=O), 1720 (C=O), 1527 (C=N), 1442 (CH $_2$ ). M.p. dec. 230 °C. HRMS [ $M^+$ ]:  $C_9H_9N_3O_3$  calc 208.0717. Found 208.1800.

1-((5-Bromofuran-2-ylmethylene)amino)imidazolidine-2,4-dione (**3c**). White solid (64% yield).  $^1H$  NMR (400 MHz, DMSO- $d_6$ )  $\delta$  ppm 11.27 (s, 1H, NH), 7.63 (s, 1H, H-6), 6.85 (d,  $J = 3.5$  Hz, 1H, H-3), 6.74 (d,  $J = 3.5$  Hz, 1H, H-4), 4.30 (s, 2H, CH $_2$ ).  $^{13}C$  NMR (101 MHz, DMSO- $d_6$ )  $\delta$  ppm 168.8, 153.3, 151.4, 132.1, 124.1, 115.5, 114.2, 48.9. Ir  $\nu$  ( $cm^{-1}$ ): 1789 (C=O), 1712 (C=O), 1481 (C=N), 1442 (CH $_2$ ). M.p. dec. 220 °C. HRMS [ $M^+$ ]:  $C_8H_6BrN_3O_3$  calc 271.9665. Found 272.0049.

1-((5-Chlorofuran-2-ylmethylene)amino)imidazolidine-2,4-dione (**3d**). White solid (89% yield).  $^1H$  NMR (400 MHz, DMSO- $d_6$ )  $\delta$  ppm 11.29 (s, 1H, NH), 7.63 (s, 1H, H-6), 6.90 (d,  $J = 3.5$  Hz, 1H, H-4), 6.65 (dd,  $J = 3.5, 1.2$  Hz, 1H, H-3), 4.31 (s, 2H).  $^{13}C$  NMR (101 MHz, DMSO)  $\delta$  169.30, 153.77, 149.73, 137.43, 132.57,

115.76, 109.83, 49.30. Ir  $\nu$  ( $cm^{-1}$ ): 1813 (C=O), 1760 (C=O), 1442 (C=N), 1350 (CH $_2$ ). M.p. 198–200 °C. HRMS [ $M^+$ ]:  $C_8H_6ClN_3O_3$  calc 228.0176. Found 228.0179.

1-((5-Nitrofur-2-ylmethylene)amino)imidazolidine-2,4-dione (nitrofurantoin) (**3e**, **NHT**). Yellow solid (95% yield).  $^1H$  NMR (400 MHz, DMSO- $d_6$ )  $\delta$  11.46 (s, 1H, NH), 7.78 (s, 1H, H-6), 7.77 (d,  $J = 3.9$  Hz, 1H, H-4), 7.13 (d,  $J = 3.9$  Hz, 1H, H-3), 4.35 (s, 2H, CH $_2$ ).  $^{13}C$  NMR (101 MHz, DMSO- $d_6$ )  $\delta$  169.1, 153.7, 152.3, 152.2, 131.6, 115.2, 115.0, 49.5. HRMS [ $M^+$ ]:  $C_8H_6N_4O_5$  calc 239.0411. Found 239.1626.

*N'*-(Furan-2-ylmethylene)benzohydrazide (**4a**). White solid (47% yield).  $^1H$  NMR (400 MHz, DMSO- $d_6$ )  $\delta$  ppm 11.79 (s, 1H, NH), 8.36 (s, 1H, H-6), 7.94–7.87 (m, 2H, H-11), 7.85 (d,  $J = 1.8$  Hz, 1H, H-5), 7.59 (t,  $J = 7.3$  Hz, 1H, H-13), 7.52 (t,  $J = 7.3$  Hz, 2H, H-12), 6.93 (d,  $J = 3.5$  Hz, 1H, H-3), 6.64 (dd,  $J = 3.5, 1.8$  Hz, 1H, C-4).  $^{13}C$  NMR (101 MHz, DMSO- $d_6$ )  $\delta$  ppm 163.1, 149.5, 145.2, 137.6, 133.4, 131.8, 128.5, 127.6, 113.5, 112.2. Ir  $\nu$  ( $cm^{-1}$ ): 3240 (N-H), 3055 (N-H), 1651 (C=O), 1473 (C=N). M.p. 180–182 °C. HRMS [ $M^+$ ]:  $C_{12}H_{10}N_2O_2$  calc 214.2205. Found 214.2215.

*N'*-(5-Methylfuran-2-ylmethylene)benzohydrazide (**4b**). White solid (98% yield).  $^1H$  NMR (400 MHz, DMSO- $d_6$ )  $\delta$  11.72 (s, 1H, NH), 8.26 (s, 1H, H-6), 7.89 (d,  $J = 7.0$  Hz, 2H, H-11), 7.58 (t,  $J = 7.3$  Hz, 1H, H-13), 7.51 (t,  $J = 7.3$  Hz, 2H, H-12), 6.81 (d,  $J = 3.2$  Hz, 1H, H-3), 6.26 (d,  $J = 3.2$  Hz, 1H, H-4), 2.34 (s, 3H, CH $_3$ ).  $^{13}C$  NMR (101 MHz, DMSO- $d_6$ )  $\delta$  163.0, 154.6, 147.9, 137.4, 133.4, 131.7, 128.4, 127.5, 115.3, 108.6, 13.5. Ir  $\nu$  ( $cm^{-1}$ ): 3210 (N-H), 3051 (N-H), 1641 (C=O), 1485 (C=N). M.p. 161–163 °C. HRMS [ $M^+$ ]:  $C_{13}H_{12}N_2O_2$  calc 228.2472. Found 228.2477.

*N'*-(5-Bromofuran-2-ylmethylene)benzohydrazide (**4c**). White solid (94% yield).  $^1H$  NMR (400 MHz, DMSO- $d_6$ )  $\delta$  ppm 11.86 (s, 1H, NH), 8.27 (s, 1H, H-6), 7.89 (d,  $J = 7.2$  Hz, 2H, H-11), 7.59 (t,  $J = 7.5$  Hz, 1H, H-13), 7.52 (t,  $J = 7.5$  Hz, 2H, H-12), 6.98 (d,  $J = 3.5$  Hz, 1H, H-4), 6.76 (d,  $J = 3.5$  Hz, 1H, H-3).  $^{13}C$  NMR (101 MHz, DMSO- $d_6$ )  $\delta$  ppm 163.1, 151.4, 136.3, 133.2, 131.8, 128.5, 127.6, 124.6, 116.2, 114.2. Ir  $\nu$  ( $cm^{-1}$ ): 3240 (N-H), 3058 (N-H), 1649 (C=O), 1475 (C=N). M.p. dec. 164 °C. HRMS [ $M^+$ ]:  $C_{12}H_9BrN_2O_2$  calc 293.1161. Found 293.1156.

*N'*-(5-Chlorofuran-2-ylmethylene)benzohydrazide (**4d**). White solid (yield 95%).  $^1H$  NMR (400 MHz, DMSO- $d_6$ )  $\delta$  11.87 (s, 1H, NH), 8.28 (s, 1H, H-6), 7.90 (d,  $J = 7.2$  Hz, 2H, H-11), 7.65–7.57 (m, 1H, H-13), 7.53 (dd,  $J = 8.2, 6.5$  Hz, 2H, H-12), 7.03 (d,  $J = 3.5$  Hz, 1H, H-4), 6.68 (d,  $J = 3.5$  Hz, 1H, H-3).  $^{13}C$  NMR (101 MHz, DMSO- $d_6$ )  $\delta$  163.60, 149.71, 137.81, 136.83, 133.70, 132.32, 128.97, 128.07, 116.41, 109.92. Ir  $\nu$  ( $cm^{-1}$ ): 3425 (N-H), 3224 (N-H), 1650 (C=O), 1489 (C=N). M.p. 170–171 °C. HRMS [ $M^+$ ]:  $C_{12}H_9ClN_2O_2$  calc 249.0431. Found 249.0435.

*N'*-(5-Nitrofur-2-ylmethylene)benzohydrazide (**4e**). Yellow solid (78% yield).  $^1H$  NMR (400 MHz, DMSO- $d_6$ )  $\delta$  ppm 12.23 (s, 1H, NH), 8.41 (s, 1H, H-6), 7.92 (d,  $J = 7.3$  Hz, 2H, H-11), 7.79 (d,  $J = 3.9$  Hz, 1H, H-4), 7.62 (t,  $J = 7.3$  Hz, 1H, H-13), 7.55 (t,  $J = 7.3$  Hz, 2H, H-12), 7.27 (d,  $J = 4.0$  Hz, 1H, H-3).  $^{13}C$  NMR (101 MHz, DMSO- $d_6$ )  $\delta$  ppm 163.5, 151.9, 151.8, 135.5, 132.8, 132.2, 128.6, 127.8, 115.3, 114.7. Ir  $\nu$  ( $cm^{-1}$ ): 3248 (N-H), 3016 (N-H), 1654 (C=O), 1475 (C=N). M.p. 221–224 °C. HRMS [ $M^+$ ]:  $C_{12}H_9N_3O_4$  calc 259.2181. Found 259.2188.

*N'*-(Furan-2-ylmethylene)-4-hydroxybenzohydrazide (**5a**). White solid (88% yield).  $^1H$  NMR (400 MHz, DMSO- $d_6$ )  $\delta$  ppm 11.58 (s, 1H, NH), 10.12 (s, 1H, OH), 8.33 (s, 1H, H-6), 7.82 (d,  $J = 1.8$  Hz, 1H, H-5), 7.81–7.75 (m, 2H, H-11), 6.89 (d,  $J = 3.4$  Hz, 1H, H-3), 6.87–6.82 (m, 2H, H-12), 6.62 (t,  $J = 3.4, 1.8$  Hz, 1H, H-4).  $^{13}C$  NMR (101 MHz, DMSO- $d_6$ )  $\delta$  ppm 162.7, 160.7, 149.6, 144.9, 136.7, 129.7, 123.8, 115.0, 113.0, 112.2. Ir  $\nu$  ( $cm^{-1}$ ): 1666 (C=O), 1435 (C=N). M.p. 230–234 °C. HRMS [ $M^+$ ]:  $C_{12}H_{10}N_2O_3$  calc 230.2199. Found 230.2211.

4-Hydroxy-*N'*-(5-methylfuran-2-yl)methylene)benzohydrazide (**5b**). White solid (97% yield).  $^1H$  NMR (400 MHz, DMSO- $d_6$ )  $\delta$

**Table 1**  
Effect of synthesized compounds on viability of different human cell lines evaluated by neutral red uptake assay.

Compound	Substituents	IC <sub>50</sub> on cell viability (μM)						
		R <sub>1</sub>	R <sub>2</sub>	HEK-293	HCT-116	HL-60	HepG2	A549
1a		H	> 500	> 500	> 500	375,0 ± 60,4	> 500	
1b		CH <sub>3</sub>	> 500	> 500	> 500	211,3 ± 19,5	471,1 ± 16,7	
1c		Br	> 500	> 500	> 500	104,5 ± 11,61	433,7 ± 26,1	
1d		Cl	> 500	> 500	> 500	> 500	> 500	
1e (NFZ)		NO <sub>2</sub>	51,8 ± 1,8	60,4 ± 3,2	23,2 ± 0,5	71,2 ± 10,5	58,5 ± 3,1	
2a		H	24,3 ± 3,8	53,3 ± 13,5	47,3 ± 2,5	62,9 ± 3,5	30,1 ± 2,0	
2b		Br	37,1 ± 1,2	50,1 ± 1,8	134,3 ± 9,3	13,2 ± 0,9	110,6 ± 7,3	
2c		NO <sub>2</sub>	6,4 ± 0,7	21,8 ± 4,2	11,4 ± 0,9	20,6 ± 2,6	4,2 ± 0,1	
3 <sup>a</sup>		H	> 500	> 500	> 500	285,1 ± 57,3	> 500	
3b		CH <sub>3</sub>	> 500	> 500	> 500	243,2 ± 21,1	> 500	
3c		Br	> 500	> 500	388,4 ± 25,7	158,9 ± 34,5	> 500	
3d		Cl	> 500	> 500	> 500	> 500	> 500	
3e (NHT)		NO <sub>2</sub>	40,4 ± 2,7	105,2 ± 7,9	40,0 ± 1,8	43,4 ± 3,1	59,9 ± 3,1	
4 <sup>a</sup>		H	> 500	> 500	> 500	420,7 ± 25,9	380,3 ± 32,5	
4b		CH <sub>3</sub>	> 500	> 500	> 500	65,6 ± 4,7	356,7 ± 16,1	
4c		Br	214,1 ± 5,1	148,7 ± 75,6	165,6 ± 4,4	82,5 ± 8,7	150,3 ± 10,4	
4d		Cl	> 500	> 500	> 500	> 500	> 500	
4e		NO <sub>2</sub>	14,6 ± 0,8	13,4 ± 0,6	17,6 ± 0,5	25,7 ± 6,5	46,7 ± 3,4	
5a		H	> 500	> 500	213,3 ± 14,7	> 500	410,9 ± 27,5	
5b		CH <sub>3</sub>	> 500	> 500	307,9 ± 10,8	> 500	309,1 ± 26,8	
5c		Br	154,3 ± 9,1	160,0 ± 7,8	9,4 ± 0,3	102,0 ± 15,1	51,7 ± 0,7	
5d		Cl	> 500	> 500	> 500	> 500	> 500	
5e (NFX)		NO <sub>2</sub>	10,9 ± 0,7	14,1 ± 0,7	7,4 ± 0,1	23,5 ± 3,4	14,4 ± 0,7	

Values are expressed as inhibitory concentration of 50% (IC<sub>50</sub>) of cell viability. NFZ: nitrofurazone; NHT: nitrofurantoin; NFX: nifuroxazide. All results correspond to the mean and s.d. of three independent experiments, performed according to methods.

11.53 (s, 1H, NH), 10.11 (s, 1H, OH), 8.24 (s, 1H, H-6), 7.80 (d,  $J = 8.7$  Hz, 2H, H-11), 6.87 (d,  $J = 8.7$  Hz, 2H, H-12), 6.75 (d,  $J = 3.3$  Hz, 1H, H-4), 6.23 (d,  $J = 3.3$  Hz, 1H, H-3), 2.32 (s, 3H, CH<sub>3</sub>). <sup>13</sup>C NMR (101 MHz, DMSO-*d*<sub>6</sub>)  $\delta$  162.7, 160.7, 154.3, 148.1, 136.7, 129.6, 123.9, 115.0, 114.8, 108.5, 13.5. Ir  $\nu$  (cm<sup>-1</sup>): 1620 (C=O), 1435 (C=N). M.p. 203–206 °C. HRMS [M<sup>+</sup>]: C<sub>13</sub>H<sub>12</sub>N<sub>2</sub>O<sub>3</sub> calc 244.2466. Found 244.2477.

*N'*-(5-Bromofuran-2-ylmethylene)-4-hydroxybenzohydrazide (**5c**). White solid (90% yield). <sup>1</sup>H NMR (400 MHz, DMSO-*d*<sub>6</sub>)  $\delta$  ppm 11.65 (s, 1H, NH), 10.13 (s, 1H, OH), 8.23 (s, 1H, H-6), 7.78 (d,  $J = 8.7$  Hz, 2H, H-11), 6.93 (d,  $J = 3.4$  Hz, 1H, H-3), 6.86 (d,  $J = 8.7$  Hz, 2H, H-12), 6.74 (d,  $J = 3.4$  Hz, 1H, H-4). <sup>13</sup>C NMR (101 MHz, DMSO-*d*<sub>6</sub>)  $\delta$  ppm 160.7, 151.6, 135.4, 129.7, 124.3, 123.7, 115.7, 115.0, 114.2. Ir  $\nu$  (cm<sup>-1</sup>): 1651 (C=O), 1442 (C=N). M.p. 198–200 °C. HRMS [M<sup>+</sup>]: C<sub>12</sub>H<sub>9</sub>BrN<sub>2</sub>O<sub>3</sub> calc 309.1155. Found 309.1164.

*N'*-(5-Chlorofuran-2-ylmethylene)-4-hydroxybenzohydrazide (**5d**). White solid (89% yield). <sup>1</sup>H NMR (400 MHz, DMSO-*d*<sub>6</sub>)  $\delta$  11.66 (s, 1H, NH), 10.14 (s, 1H, OH), 8.24 (s, 1H, H-6), 7.83–7.75 (m, 2H, H-11), 6.98 (d,  $J = 3.5$  Hz, 1H, H-3), 6.91–6.83 (m, 2H, H-12), 6.66 (d,  $J = 3.5$  Hz, 1H, H-4). <sup>13</sup>C NMR (101 MHz, DMSO-*d*<sub>6</sub>)  $\delta$  163.25, 161.23, 149.90, 137.54, 135.95, 130.16, 124.13, 115.86, 115.51,

109.84. Ir  $\nu$  (cm<sup>-1</sup>): 1635 (C=O), 1435 (C=N). M.p. 186–188 °C. HRMS [M<sup>+</sup>]: C<sub>12</sub>H<sub>9</sub>ClN<sub>2</sub>O<sub>3</sub> calc 265.0380. Found 265.0383.

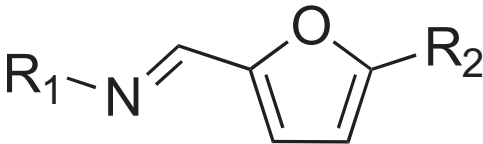
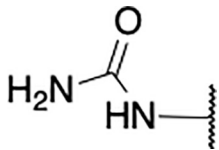
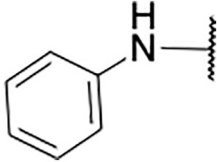
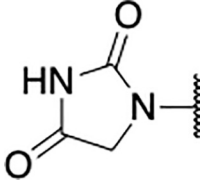
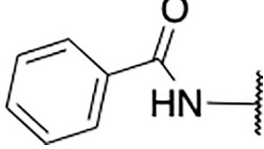
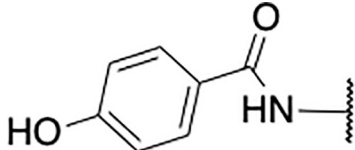
4-Hydroxy-*N'*-((5-nitrofuran-2-yl)methylene)benzohydrazide (nifuroxazide) (**5e**, NFX). Yellow solid (65% yield). <sup>1</sup>H NMR (400 MHz, DMSO-*d*<sub>6</sub>)  $\delta$  ppm 12.03 (s, 1H, NH), 10.22 (s, 1H, OH), 8.37 (s, 1H, H-6), 7.81 (d,  $J = 8.6$  Hz, 2H, H-11), 7.78 (d,  $J = 3.9$  Hz, 1H, H-4), 7.23 (d,  $J = 3.9$  Hz, 1H, H-3), 6.88 (d,  $J = 8.6$  Hz, 2H, H-12). <sup>13</sup>C NMR (101 MHz, DMSO-*d*<sub>6</sub>)  $\delta$  ppm 161.3, 161.1, 152.1, 151.8, 130.0, 123.2, 115.3, 115.1, 114.8, 114.7. Ir  $\nu$  (cm<sup>-1</sup>): 1674 (C=O), 1465 (C=N). M.p. dec. 257 °C. HRMS [M<sup>+</sup>]: C<sub>12</sub>H<sub>9</sub>N<sub>3</sub>O<sub>5</sub> calc 275.2176. Found 275.2192.

## 2.2. Pharmacology

### 2.2.1. Materials

Cell media, non-essential aminoacids, penicillin-streptomycin, trypsin, and fetal bovine serum were obtained from Biological Industries (Israel). HBSS, PBS, Neutral Red, Dichlorofluorescein diacetate, 1-chloro-2,4-dinitrobenzene, reduced glutathione, Pyrogallol Red (PGR),  $\beta$ -NADPH, glucose-6-phosphate, glucose-6-phosphate dehydrogenase (from *Saccharomyces cerevisiae*) were purchased from Sigma-Aldrich. MTT was obtained from AkSci (USA).

**Table 2**  
Effect of synthesized compounds on cytosolic GST activity.

Compound	Substituents		IC <sub>50</sub> on GST activity (μM)
	R <sub>1</sub>	R <sub>2</sub>	
			
1a		H	n.i.
1b		CH <sub>3</sub>	n.i.
1c		Br	n.i.
1d		Cl	n.i.
1e		NO <sub>2</sub>	157,0 ± 7,4
(NFZ)			
2a		H	168,0 ± 23,9
2b		Br	n.d.
2c		NO <sub>2</sub>	n.d.
			
3a		H	n.i.
3b		CH <sub>3</sub>	n.i.
3c		Br	n.i.
3d		Cl	n.i.
3e		NO <sub>2</sub>	136,4 ± 6,1
(NHT)			
4a		H	n.i.
4b		CH <sub>3</sub>	128,4 ± 10,0
4c		Br	197,8 ± 18,8
4d		Cl	98,7 ± 10,1
4e		NO <sub>2</sub>	n.d.
			
5a		H	n.i.
5b		CH <sub>3</sub>	n.i.
5c		Br	153,6 ± 19,7
5d		Cl	n.i.
5e		NO <sub>2</sub>	n.d.
(NFX)			

Values are expressed as inhibitory concentration on GST activity. (n.i.: no inhibition). (n.d.: not determined due solubility problems). NFZ: nitrofurazone, NHT: nitrofurantoin, NFX: nifuroxazide. All results are expressed in mean and s.d., as result of three independent experiments.

### 2.2.2. Cell cultures

Human cancer cell lines HTC116 and HL60 cells were maintained in RPMI 1640 medium; HepG2, A549 and Hek293 were maintained in DMEM medium. Media was supplemented with Fetal Bovine Serum (5% for assays and 10% for growth), 1× non-essential aminoacids and 100 U/ml penicillin and 100 μg/ml streptomycin. All cells were cultured in a humidified incubator at 5% CO<sub>2</sub> atmosphere and 37 °C.

### 2.2.3. Calculation of consensus octanol-water partition coefficient:

The LogP<sub>o/w</sub> values of synthesized derivatives was calculated using the free software SwissADME (developed by the Swiss Institute of Bioinformatics). This computational tool gives a coefficient value named consensus LogP (cLogP), obtained through the arithmetic media of 5 different theoretical calculations: XLOGP3, WLOGP, MLOGP, SILICOS-IT e iLOGP (Daina et al., 2017).

### 2.2.4. Cell viability studies by Neutral Red Uptake Assay

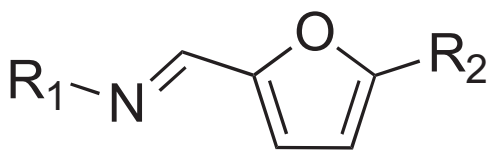
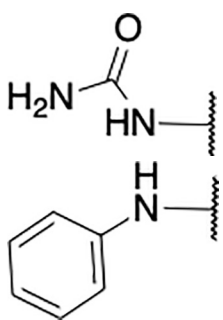
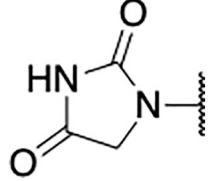
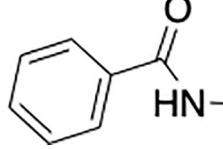
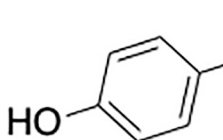
Briefly, cell lines were seeded in 96-well flat bottom plate at 1 × 10<sup>4</sup> cell per well density in 100 μl of corresponding media supplemented with 5% FBS. Cells were incubated overnight and afterwards, different concentrations of compounds (1 to 500 μM, in DMSO

maintaining a maximum concentration of 1% v/v) were added. Compounds were incubated for 72 h in a humidified incubator at 5% CO<sub>2</sub> and 37 °C. After incubation, viability assays were performed according to previous reported methodology with some modifications (Repetto et al., 2008). Briefly, media was removed of each plate and 100 μl of 2 μg/ml Neutral Red solution in corresponding media was added to each well. Cells were incubated for 3 h at 37 °C, gently washed three times with PBS 1× and then acidified alcoholic solution was added to extract the incorporated dye. Fluorescence was measured with an excitation and emission wavelengths of 580/620 nm respectively using a Biotek® Cytation5 reader.

### 2.2.5. Evaluation of antibacterial activity

MIC determination on *Escherichia coli* and *Staphylococcus aureus* was determined using a broth microdilution method according to recommendations of the Clinical and Laboratory Standards Institute (CLSI, 2003). Briefly, bacteria were cultured for 24 h before the experiments were carried out. All compounds were dissolved in DMSO (not exceeding 1% v/v) and diluted in media. An inoculum of 5 × 10<sup>5</sup> CFU/ml was seeded in 96-well U-shaped plates, compounds added and incubated for 24 h at 37 °C. Finally, MIC was determined in the

**Table 3**  
Minimal Inhibitory Concentration of synthesized compounds evaluated on two different bacterial strains.

Compound	Substituents		MIC on bacterial strains ( $\mu\text{g/ml}$ )	
	R <sub>1</sub>	R <sub>2</sub>	<i>E. coli</i>	<i>S. aureus</i>
1a		H	> 64	> 64
1b		CH <sub>3</sub>	> 64	> 64
1c		Br	> 64	> 64
1d		Cl	> 64	> 64
1e		NO <sub>2</sub>	8	16
(NFZ)				
2a		H	> 64	> 64
2b		Br	> 64	> 64
2c		NO <sub>2</sub>	> 32	> 32
3a		H	> 64	> 64
3b		CH <sub>3</sub>	> 64	> 64
3c		Br	> 64	> 64
3d		Cl	> 64	> 64
3e		NO <sub>2</sub>	8	16
(NHT)				
4a		H	> 64	> 64
4b		CH <sub>3</sub>	> 64	> 64
4c		Br	> 64	> 64
4d		Cl	> 64	> 64
4e		NO <sub>2</sub>	> 32	> 32
5a		H	> 64	> 64
5b		CH <sub>3</sub>	> 64	> 64
5c		Br	> 64	> 64
5d		Cl	> 64	> 64
5e		NO <sub>2</sub>	32	8
(NFX)				

Compounds were evaluated in serial dilutions starting at 64 mg/ml (less soluble compounds started at 32 mg/ml). NFZ: nitrofurazone; NHT: nitrofurantoin; NFX: nifuroxazide. All results correspond to the MIC observed in three independent experiments.

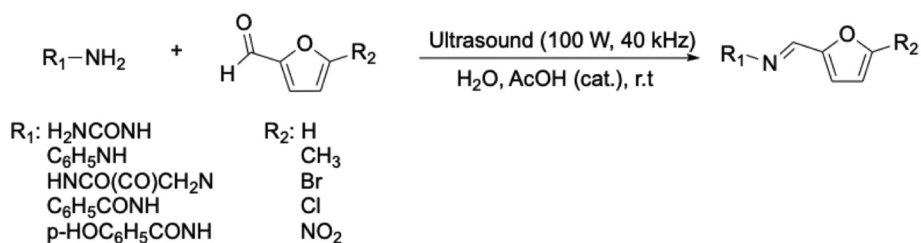


**Fig. 1.** Route of synthesis of 2,5-disubstituted furans.

corresponding dilution where no visible growth of bacteria was observed. Gentamycin and Vancomycin were also tested against *E. coli* and *S. aureus* and results compared to MIC ranges reported by the CLSI, as a quality control measure.

#### 2.2.6. Preparation of rat liver microsomes and cytosol

Microsomes and cytosol were donated by Prof. María Eugenia Letelier. Preparation was performed as previously described (Letelier et al., 2004). Adult male Sprague-Dawley rats (200–300 g), maintained at the vivarium of the Facultad de Ciencias Químicas y Farmacéuticas

(Universidad de Chile, Santiago, Chile) were used. Rats were allowed free access to pelleted food, maintained at controlled temperature (22 °C), and photoperiod (lights on from 07:00 to 19:00 h). All procedures were carried out using protocols approved by Institutional Ethical Committees of the Facultad de Ciencias Químicas y Farmacéuticas, Universidad de Chile, and Facultad de Química, Pontificia Universidad Católica de Chile, and according to the guidelines of the Guide for the Care and Use of Laboratory Animals (NCR, USA). Animals were fasted for 15 h with water *ad libitum* and sacrificed by decapitation. Livers were perfused *in situ* with 4 vol of 25 ml 0.9% (w/v) NaCl, excised, and



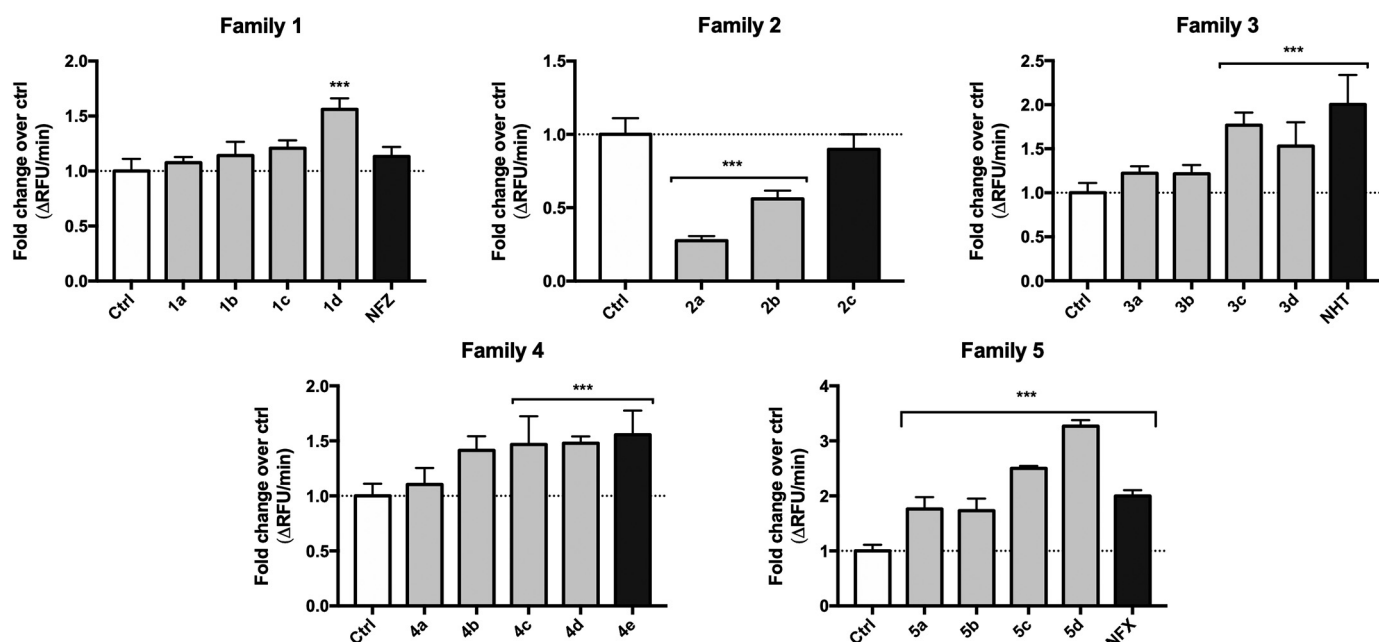


Fig. 2. Intracellular ROS generation in HepG2 cell line. Cells were pre-loaded with DCFDA and then exposed to the synthesized compounds at a concentration of 50  $\mu$ M for 1 h. Bars represent the ratio of fluorescence generation of experiments over time and fluorescence generation of control over time, expressed as the mean and standard deviation of three independent experiments. Significant differences were considered when  $p < .05$  (\*\*\*) by ANOVA test using GraphPad Prism 7.0.

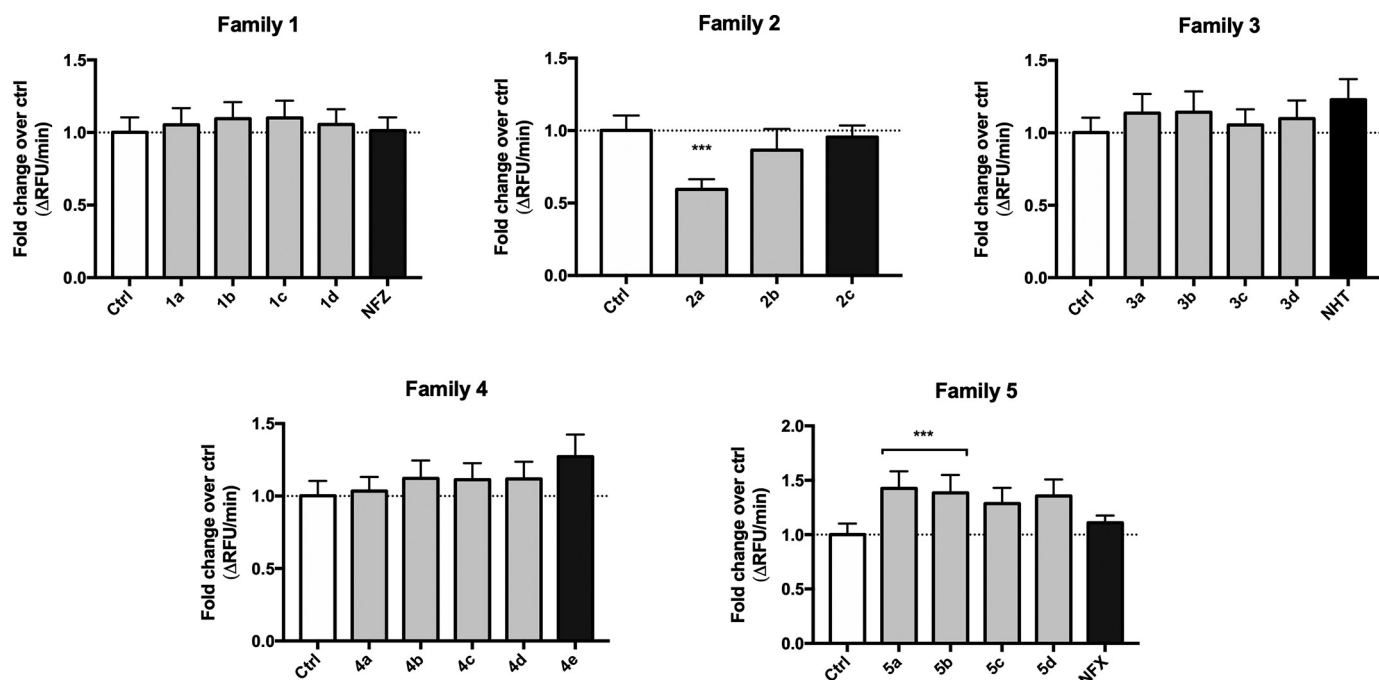


Fig. 3. Intracellular ROS generation in HL60 cell line. Cells were pre-loaded with DCFDA and then exposed to the synthesized compounds at a concentration of 50  $\mu$ M for 1 h. Bars represent the ratio of fluorescence generation of experiments over time and fluorescence generation of control over time, expressed as the mean and standard deviation of three independent experiments. Significant differences were considered when  $p < .05$  (\*\*\*) by ANOVA test using GraphPad Prism 7.0.

placed on ice. All homogenization and fractionation procedures were performed at 4  $^{\circ}$ C and all centrifugations were performed using either a Suprafuge 22 Heraeus centrifuge or an XL-90 Beckmann ultracentrifuge. Liver tissue (9–11 g wet weight), devoid of connective and vascular tissue, was homogenized with 5 vol of 0.154 M KCl, with eight strokes in a Dounce Wheaton B homogenizer. Homogenates were centrifuged at 9000 g for 15 min and sediments discarded. Supernatants were centrifuged at 105,000 g for 60 min. Sediments (microsomes,

enriched in endoplasmic reticulum) and supernatants (cytosol) were stored at  $-80$   $^{\circ}$ C until use. Protein determinations were performed according to Lowry method (Lowry et al., 1951).

#### 2.2.7. Bleaching of PGR induced by $O_2^{\cdot -}$

The consumption of PGR mediated by  $O_2^{\cdot -}$  generated by nitrofurantoin-induced redox cycling was measured as previously described (Faúndez et al., 2011). Briefly, a reaction mixture containing microsomal protein

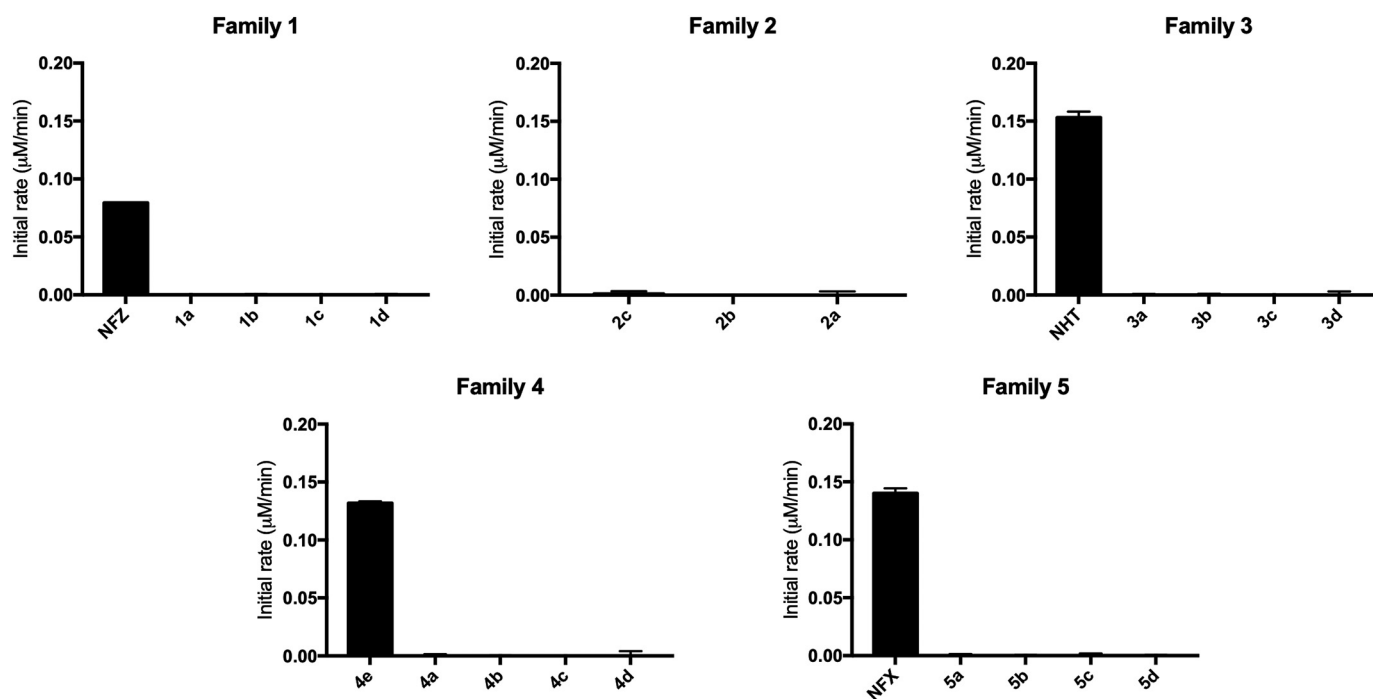


**Fig. 4.** Superoxide generation induced by cytochrome P450 reductase. Rat liver microsomes were incubated with synthesized compounds at a concentration of 250  $\mu\text{M}$ . Initial rate of consumption of PGR was quantified and converted to superoxide anions equivalents. Bars correspond to the meaning of three independent experiments.

(10–150  $\mu\text{g}/\text{ml}$ ), KCN (1 mM), glucose 6-phosphate (6 mM), NADP (0.6 mM), G-6-P dehydrogenase (5 U/ml) (named from hereon as microsomal system (MS)), plus PGR (10  $\mu\text{M}$ ) and compounds (100  $\mu\text{M}$ ) in phosphate buffer (50 mM, pH 7.4) was incubated at 37  $^{\circ}\text{C}$ . The reaction was initiated by the addition of G-6-P dehydrogenase and nitroreduction assessed by the bleaching in the absorbance of PGR at 540 nm using a Jenway 6705 UV/Vis spectrophotometer.

#### 2.2.8. Kinetic analysis of intracellular ROS generation

Determination of intracellular ROS generation was performed according to Wolfe and Rui (2007). Briefly, HepG2 and HL60 cells were seeded in 96-well flat bottom fluorescence plates in a  $5 \times 10^4$  cells per well density in DMEM and RPMI, respectively, with 5% FBS and left overnight. Media was removed and replaced with fresh un-supplemented media with 20  $\mu\text{M}$  of DCFDA. HL60 cells were incubated with DCFDA previous to seeding in the plates. After incubation, cells were washed twice with sterile HBSS and then compounds were added. Fluorescence generation was measured every 2 min for 1 h with excitation/emission wavelengths of 480/520 respectively in a Biotek<sup>®</sup> Cytation5 reader. Results are expressed as fold changes of fluorescence generation under each condition over time, normalized to fluorescence generation by the control over time (slope of condition/slope of control).

#### 2.2.9. Assays of cytosolic GST activity

Conjugation of 1-chloro-2,4-dinitrobenzene with GSH, reaction catalyzed by GST, was assayed as previously described (Letelier et al., 2010). For each condition, 10  $\mu\text{g}$  of cytosolic protein, 1-chloro-2,4-dinitrobenzene and GSH as substrates (1 and 4 mM final concentration, respectively) and different concentrations of compounds (1 to 500  $\mu\text{M}$ , in DMSO with a maximum concentration of 1% v/v of solvent) were added in 100 mM sodium phosphate buffer, pH 6.5. Compounds were incubated for 1 h before GSH was added. Conjugated-substrate apparition was continuously recorded for 2 min at 25  $^{\circ}\text{C}$ , immediately after GSH was added to initiate the reaction, at 340 nm ( $\epsilon_{340} = 9.6 \text{ mM}^{-1} \text{ cm}^{-1}$ ) in a Jenway<sup>®</sup> 6705 UV-VIS

spectrophotometer. All GST activity assays were performed in conditions of linearity respect to incubation time and protein concentration.

#### 2.2.10. Inhibition mechanism of nitrofurantoin on GST activity

In order to determine the mechanism of inhibition of nitrofurantoin on cytosolic GST, hepatic cytosol was incubated for 1 h with different concentrations of nitrofurantoin and then enzymatic assays were performed with increasing concentrations of GSH (at a CDNB concentration of 1 mM) and increasing concentrations of CDNB (at a GSH concentration of 4 mM), according to methods. Inhibition mechanisms were determined using the software GraphPad<sup>®</sup> Prism 7.0.

### 2.3. Statistical analysis

Each result corresponds to the mean of three independent experiment performed with 3 replicates per condition. All statistical analyses were performed using the software GraphPad<sup>®</sup> Prism version 7.0.

## 3. Results

### 3.1. Effect of synthesized derivatives on cell viability

In order to determinate the cytotoxic profile of derivatives,  $\text{IC}_{50}$  value (concentration that induce a decrease of 50% on cell viability) was determined using neutral red uptake assay. Depending on solubility, cells were incubated with concentrations of the compounds up to 500 or 250  $\mu\text{M}$ . Nitrofurantoin derivatives were found to be the most toxic, among all the synthesized compounds (Table 1). According with our hypothesis, 5-nitro group substitution did not suppress totality the toxicity of derivatives. Halogenated bromine and nitrofurantoin derivatives displayed a similar  $\text{IC}_{50}$  values on HepG2 cell line viability. Compounds from family 2 were the most toxic among all derivatives, where nitro (2c), hydrogen (2a) or bromine (2b) in position 5 of the furan ring exhibited similar  $\text{IC}_{50}$  values among all cell lines (Table 1). In order to predict if the chemical substitutions of nitro group and the observed variations in cytotoxicity values ( $\text{IC}_{50}$ ) were affected by membrane



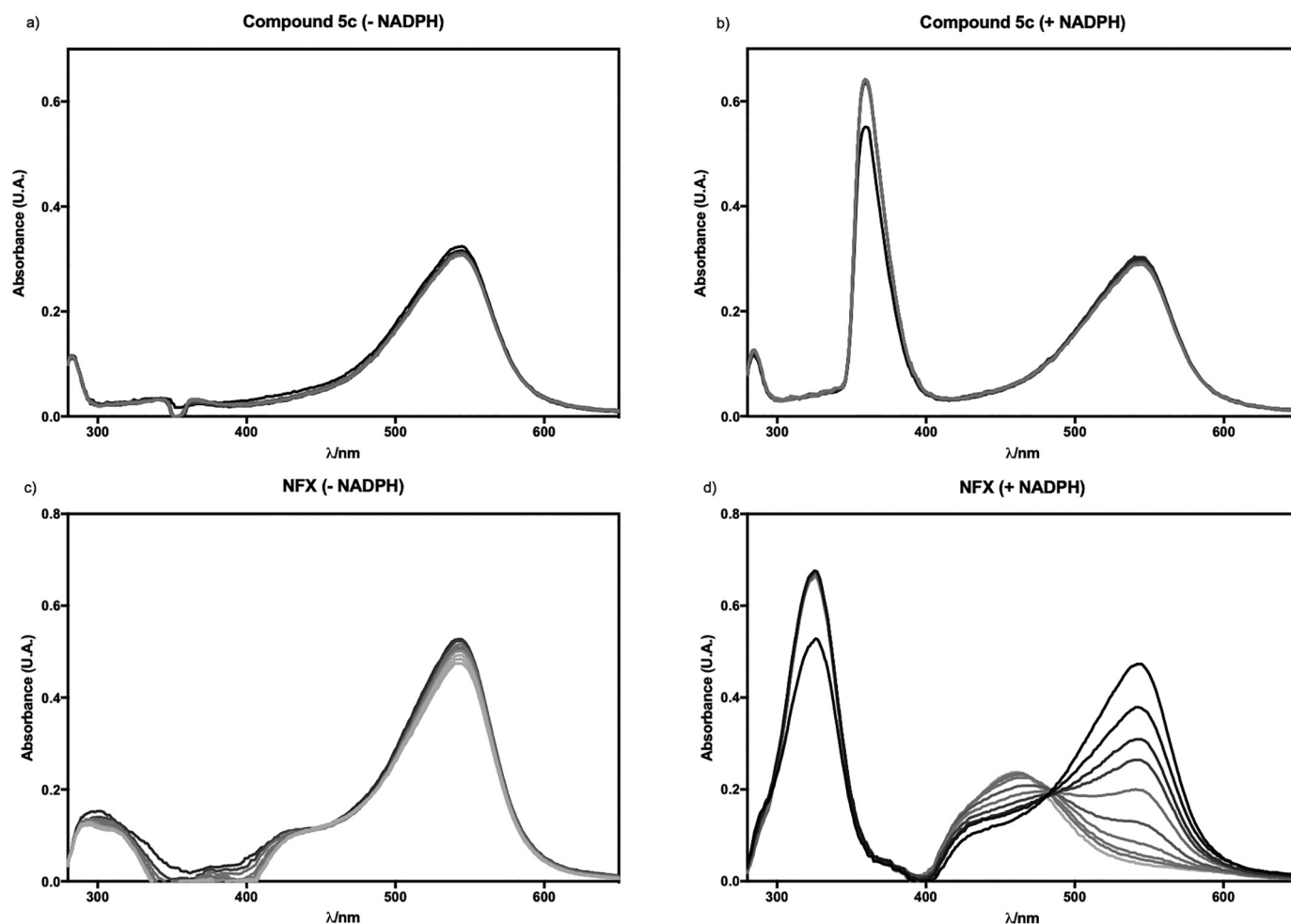


Fig. 5. Spectra of PGR reduction. PGR bleaching by superoxide is characterized by spectral changes, as displayed in the lower figures c and d. Two representative compounds of the same family were chosen (Brominated 5c and nifuroxazide NFX). Compounds at 250  $\mu$ M were incubated with microsomal system (a and c) and NADPH was added to the system (b and d).

permeability, the consensus octanol-water partition coefficient was calculated (Table 2 in the Supplementary Material). Non-significant changes in cLogP values were observed into a chemical family when nitro group was substituted by  $-H$ ,  $-CH_3$ ,  $-Cl$  or  $-Br$  suggesting that these substitutions are not affecting membrane permeability and therefore, the observed cytotoxicity  $IC_{50}$  can be attributed to pharmacodynamics exclusively.”

### 3.2. Intracellular ROS generation induced by synthesized derivatives in cell lines

It is widely accepted that one electron reduction of 5-nitrogroup and the consequent ROS generation could be the source of its toxic effects. With the aim to determinate the contribution of the nitro group to cellular oxidative stress, intracellular ROS generation was determined using cells pre-loaded with DCFDA which were incubated for 1 h with 50  $\mu$ M of the synthesized compounds and then fluorescence was measured as described in methods. The results show that ROS generation was independent of the presence of a nitrogroup (Figs. 2 and 3). Halogenated derivatives of families 4 and 5 (compounds 4c-d and 5c-d) were found to generate as much ROS as their nitro counterpart. Surprisingly, compounds belonging to family 2 did not generate intracellular ROS despite being among the most cytotoxic agents. These results suggest that there are mechanisms of ROS generation independent of the presence of the 5-nitro group in the furan ring.

### 3.3. Bleaching of PGR induced by superoxide anion radicals generated by redox cycling of derivatives in rat liver microsomes

It is well known that nitro-containing drugs, as nitrofurans, can enter into redox cycling in a reaction catalyzed by enzymes with nitroreductase activity, mainly NAD(P)H-cytochrome P450 reductase in mammals. With the purpose of determining the capacity of the synthesized derivatives to generate ROS catalyzed by NAD(P)H-cytochrome P450 reductase, rat liver microsomes were incubated with the synthesized derivatives and bleaching of pyrogallol red was evaluated according to methods. In the experimental conditions, this probe reacts specifically with superoxide anion radical which allows to determine the generation of this radical through redox cycling (Atala et al., 2013). Results demonstrate that only nitro-containing compounds are able to generate superoxide anion radical through cytochrome P450 reductase, indicating that only the 5-nitro group is able to generate ROS through enzymatic reduction. Nonetheless, it was observed that nitrofuran derivative compound 2c was not able to generate superoxide (Fig. 4). These results support the idea that cytotoxicity of 2-hydrazonylfuran derivatives is not fully dependent on ROS generation induced by nitroreduction.

### 3.4. Maps of electrostatic potential of synthesized compounds

In order to gain further insight into the chemical changes induced by the structural modifications in the compounds, the MEP of each

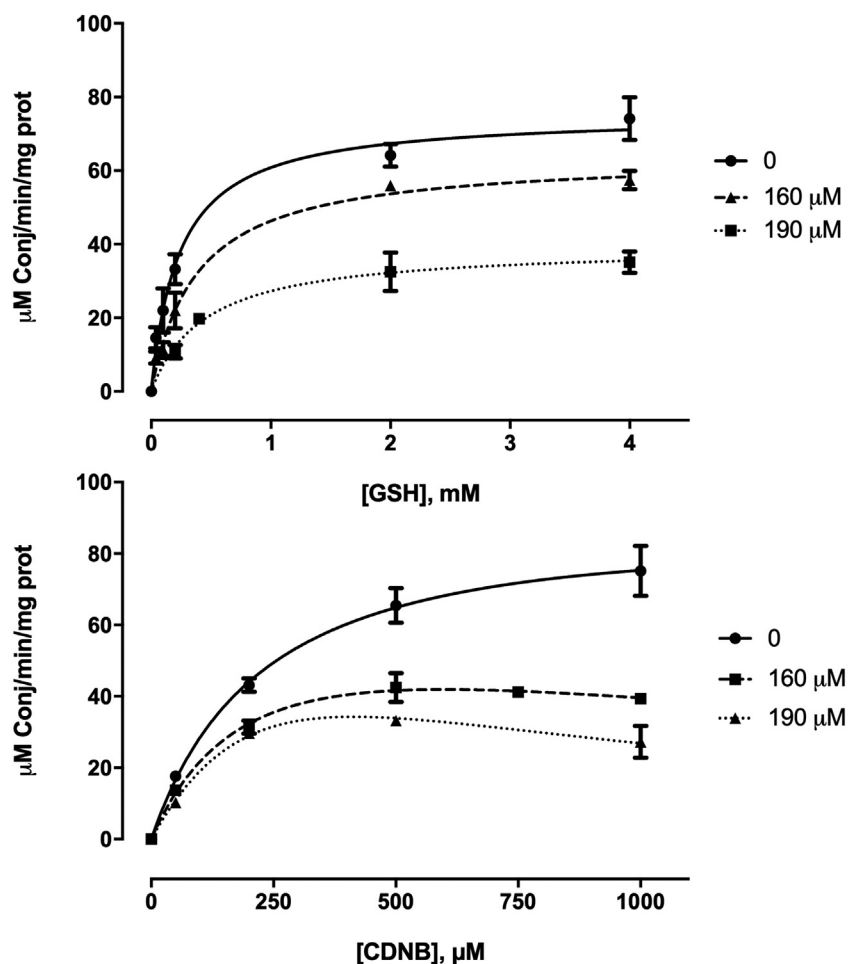


**Fig. 6.** Inhibition mechanism of nitrofurantoin on GST activity. Rat liver cytosol was incubated with two different concentrations of nitrofurantoin (160 and 190  $\mu\text{M}$ ) and increasing concentrations of substrates CDNB (top figure) and GSH (Bottom figure) were added. Each point represents the meaning and s.d. of at least two independent experiments. Kinetics parameters  $K_m$  and  $V_m$  determination by non-linear regression using GraphPad Prism 7.0.

molecule was calculated and analyzed. As can be expected, the electron density over the furan ring varies according to the substituent on the heterocyclic ring in the order of  $\text{NO}_2 < \text{Cl} < \text{Br} < \text{H} < \text{CH}_3$  with  $\text{NO}_2$  group leaving the least electron density and the Methyl group the greatest electron density on the furan ring. This pattern was repeated among all families synthesized (Supplementary material, see along row). Also, the withdrawing effect of the substituents is transmitted along the molecule, affecting the density over the carboxamide/hydrazide/hydrazine/hydantoin moiety, although not as pronounced as in the furan ring. Comparing the MEP results between families (Supplementary material, see along column), the electronic density over the furan ring remains comparable between families except for family 2 compounds which presents higher electron densities compared to the other families. However, when analyzing the opposite moieties to the furan ring of synthesized compounds, the electron density varies from low (hydantoin, family 3) to neutral (carboxamide, family 1) and high (hydrazine, family 2, hydrazide, families 4 and 5) indicating the presence of both electron-poor and electron-rich groups. These results, along with viability assay results, suggest that the electron-density on this portion of the molecules should not influence cellular toxicity.

### 3.5. Effect of derivatives on cytosolic GST activity

Given the intracellular ROS generation and the lipophilic and electrophilic characteristics of the nitrofurans and their synthesized derivatives, we evaluated their effect on glutathione S-transferase activity.

Cytosolic GST activity was inhibited by nitrofurazone (NHT) ( $\text{IC}_{50}$ : 139,6  $\mu\text{M}$ ), nitrofurantoin (NFZ) ( $\text{IC}_{50}$ : 136,4  $\mu\text{M}$ ), and nifuroxazide (NFX) (solubility problem to obtain an  $\text{IC}_{50}$  value) (Table 2). The brominated derivative of nifuroxazide compound 5c was able to inhibit GST activity in a concentration-response manner similar to its nitro counterpart, with an  $\text{IC}_{50}$  of 153,6  $\mu\text{M}$ . Methyl and hydrogen derivatives (1a-b, 3a-b, 4a, and 5a-b) did not inhibit GST activity despite the time of incubation, excepting compound 4b which exhibited an  $\text{IC}_{50}$  of 128,4  $\mu\text{M}$ . Family 2 had no effect on GST activity, except for compound 2a with an  $\text{IC}_{50}$  of 168,0  $\mu\text{M}$ .

### 3.6. Inhibition mechanism of nitrofurantoin on liver cytosolic GST activity

Nitrofurantoin remains as one of the most used drugs in the treatment of urinary tract infections due to its low resistance generation and high effectiveness. Given that nitrofurantoin was able to inhibit cytosolic GST activity in a concentration-dependent manner, we decided to determine its inhibition mechanisms on GST activity. Results indicate that nitrofurantoin inhibited GST activity in a non-competitive mechanism respect to GSH, and *via* a substrate-inhibition mechanism respect to CDNB (Fig. 6).

### 3.7. Antibacterial activity of synthesized compounds

The antibacterial and antiparasitic activity of the nitrofurans is due to a metabolic reduction of the 5-nitro group, therefore all the synthesized compounds were evaluated for their antibacterial activity. As

expected, the non-nitrated compounds did not show antibacterial activity in aerobic conditions against *E. coli* and *S. aureus* in concentrations less than 64 µg/ml (Table 3). Surprisingly, compound **2c**, despite being a nitrofurantoin, did not show antibacterial activity.

#### 4. Discussion

The 5-nitro-2-hydrazonefuran scaffold is conserved in all nitrofurantoin drugs, i.e. nitrofurazone, nitrofurantoin, nifuroxazide, furazolidone and nifurtimox. Here, we synthesized non-nitrated derivatives of nitrofurazone, nitrofurantoin and nifuroxazide in order to determine the contribution of the parental skeleton on cell toxicity aside from reduction of the 5-nitro group (Fig. 1). Our first proposal was to obtain the amino derivatives of nitrofurans, but it was certainly difficult. We corroborated that reduction of 5-nitrofurans using traditional methods (catalytic hydrogenation, metal-hydrides and metal in acidic medium) was not successful: compounds decomposed by ring opening (Ebetino et al., 1962; LARGERON and Fleury, 1991; Pessoa-Mahana et al., 2005). As no positive results were obtained, we decided to synthesize derivatives with different chemical characteristics.

Cell viability results indicated that the presence of electron withdrawing and lipophilic substituent groups, such as nitro and bromine, increase the toxicity compared to electron donor methyl group or unsubstituted furan ring. Toxicity of nitrofurantoin derivatives can be explained through the canonical mechanism attributed to nitrofurantoin drugs, i.e. redox cycling and ROS generation, but these considerations are not valid for non-nitrated derivatives. Intracellular ROS generation experiments surprisingly showed that bromine and chlorine derivatives **4c-d** and **5c-d** were able to generate as much intracellular ROS as the nitro-substituted counterpart in hepatic cell line (Fig. 2). These results suggest that the ROS generation is independent of the presence of the nitro group, and therefore independent of nitroreduction. More unexpectedly, derivatives from family 2, the most toxic of all synthesized compounds did not generate intracellular ROS as would be expected, especially for nitro derivative **2c** (Figs. 2 and 3). As it is widely known, cytochrome P450 reductase has been attributed as the main source of superoxide generation, induced by redox cycling in nitrofurans. Given that only derivatives containing a nitro group could generate superoxide anion through cytochrome P450 reductase, we decided to incubate microsomes with all the synthesized derivatives. As expected, nitrofurans generated superoxide anion through cytochrome P450 reductase in different extents (Fig. 4), probably due to contributions of the substituents in position 2 of the furan ring (Morales et al., 1987). Non-nitrated compounds did not generate superoxide anion, but surprisingly neither nitroderivative **2c** was nitroreduced by cytochrome P450 reductase (Fig. 4). These results could be explained based on the electronic properties of the 2-hydrazonefuran portion of these derivatives. Among all families, family 2 exhibited the higher electronic density on furan ring. There are reports that correlate the nitroreduction ability with their electronic density, indicating that the lesser the electronic density, the greatest is the nitroreduction (Morales et al., 1987; Núñez-Vergara et al., 2000; Olive, 1979). It is possible that due to the higher electronic density in the furan ring, and therefore the decreased electrophilicity of the nitro group, the nitroreduction in derivative **2c** is electronically impeded due to instability of intermediaries. Therefore, these electronic phenomena allow us to explain the inefficacy of **2c** to generate intracellular ROS. In a similar manner, nitrocompounds in bacteria undergo two-electron reduction catalyzed by Type 1 nitroreductases, this phenomenon generates nitroso and hydroxylamine metabolites that can impair protein synthesis in the microorganism. Our results showed that compound **2c** was unable to exert a bacteriostatic effect suggesting that Type 1 nitroreductases are unable to reduce the 5-nitro group in a furan ring with high electronic density. All these results allow us to propose that C-5 electron donor substituent in the furan rings coupled to the 2-hydrazone moiety confer differential toxicity on eukaryotic cells and have no effect on bacterial

microorganism. This proposal will be checked it out in oncoming research (Fig. 5). (See Fig. 5.)

At this point, our results suggest that nitroreduction and ROS generation are not the only responsible mechanisms of cellular toxicity. Halogenated derivatives were toxic in different degrees, but even more important, family 2 was found to be the most cytotoxic among all families despite their lack of generation of intracellular ROS or reduction by cytochrome P450 reductase.

Based on MEP calculations that showed highly electrophilic areas in azomethine moiety, and previous reports in bacteria (Perito et al., 1996), we decided to evaluate the effect of compounds on hepatic cytosolic GST activity. Our results on hepatic cytosol indicate that nitrofurantoin inhibit GST activity with an  $IC_{50} = 136,4 \mu M$  in a non-competitive mechanism for enzyme substrates GSH and CDNB (Table 2 and Fig. 6). There is no evidence of nitrofurans conjugated with GSH catalyzed by GST (Asaoka and Takahashi, 1989). However, it was previously demonstrated that nitrofurantoin inhibited GSTB1-1 from *P. mirabilis* ( $IC_{50} = 140 \mu M$ ) (Perito et al., 1996). Kinetic parameters,  $k_{cat}$  and  $K_m$ , for GSH and CDNB were modified suggesting a non-competitive inhibition mechanism for both substrates. The GSTB1-1 from *P. mirabilis* shows a low sequence identity to mammalian GSTs, but despite this lack in sequence similarity, three-dimensional structure is common for bacterial and mammalian GSTs (Perito et al., 1996). The latter might explain the similarity in the GST inhibition results on the nitrofurantoin activity, and its potential inhibition mechanisms for these enzymes. However, these compounds might also be affecting other GSH-dependent enzymatic systems such as GSH-reductases, glutamate cysteine ligase, glutathione peroxidases and others. For this reason, the possible effect of the series compound on these targets will be evaluated in our laboratory.

In conclusion, the obtained results may allow us to conclude that nitrofurans cytotoxicity is not fully dependent on oxidative stress induced by ROS generation and/or nitroreduction. These findings should be taken in consideration for future designs of 5-nitrofurantoin derivatives and clinical studies.

#### Declaration of Competing Interest

The authors declare that they have no known competing financial interests or personal relationships that could have appeared to influence the work reported in this paper.

#### Acknowledgements

Thanks to professor María Eugenia Letelier (R.I.P.) for donating rat liver microsomes and cytosol.

This research was supported by the following grants: Fondecyt EQM 160042 (Pontificia Universidad Católica de Chile); Fondecyt 1170269 (H. Pessoa-Mahana); Beca Doctorado Nacional Conicyt 21170382 (C. Gallardo-Garrido); and DIPOG 2018 (M. Faúndez).

#### Appendix A. Supplementary data

Supplementary data to this article can be found online at <https://doi.org/10.1016/j.taap.2020.115104>.

#### References

- (ESCMID), E.C. for A.S.T. (EUCAST) of the E.S. of C.M. and I.D., 2003. Determination of minimum inhibitory concentrations (MICs) of antibacterial agents by broth dilution. Clin. Microbiol. Infect. 9, ix–xv. <https://doi.org/10.1046/j.1469-0691.2003.00790.x>.
- Asaoka, K., Takahashi, K., 1989. Glutathione conjugation of nitro compounds by monkey glutathione S-transferases. Biochem. Pharmacol. 38, 2977–2983. [https://doi.org/10.1016/0006-2952\(89\)90005-1](https://doi.org/10.1016/0006-2952(89)90005-1).
- Atala, E., Velásquez, G., Vergara, C., Mardones, C., Reyes, J., Tapia, R.A., Quina, F., Mendes, M.A., Speisky, H., Lissi, E., Ureta-Zañartu, M.S., Aspée, A., López-Alarcón, C., 2013. Mechanism of pyrogallol red oxidation induced by free radicals and reactive

- oxidant species. A kinetic and spectroelectrochemistry study. *J. Phys. Chem. B* 117, 4870–4879. <https://doi.org/10.1021/jp400423w>.
- Castro, J.A., de Mecca, M.M., Bartel, L.C., DeMecca, M.M., Bartel, L.C., de Mecca, M.M., Bartel, L.C., 2006. Toxic side effects of drugs used to treat Chagas' disease (American Trypanosomiasis). *Hum. Exp. Toxicol.* 25, 471–479. <https://doi.org/10.1191/0960327106het653oa>.
- Daina, A., Michielin, O., Zoete, V., 2017. SwissADME: a free web tool to evaluate pharmacokinetics, drug-likeness and medicinal chemistry friendliness of small molecules. *Sci. Rep.* 7, 42717. <https://doi.org/10.1038/srep42717>.
- Dershwitz, M., Novak, R.F., 1980. Lack of inhibition of glutathione reductase by un-nitrated derivatives of nitrofurantoin. *Biochem. Biophys. Res. Commun.* 92, 1313–1319.
- Dershwitz, M., Novak, R.F., 1982. Studies on the mechanism of Nitrofurantoin-mediated red cell toxicity. *J. Pharmacol. Exp. Ther.* 222, 430–434.
- Ebetino, F.F., Carroll, J.J., Gever, G., 1962. Reduction of Nitrofurans. I. Aminofurans. *J. Med. Pharm. Chem.* 5, 513–524. <https://doi.org/10.1021/jm01238a011>.
- Faúndez, M., Rojas, M., Bohle, P., Reyes, C., Letelier, M.E., Aliaga, M.E., Speisky, H., Lissi, E., López-Alarcón, C., 2011. Pyrogallol red oxidation induced by superoxide radicals: application to evaluate redox cycling of nitro compounds. *Anal. Biochem.* 419, 284–291. <https://doi.org/10.1016/j.ab.2011.08.048>.
- Goemaere, N.N.T., Grijm, K., van Hal, P.T.W., den Bakker, M.A., 2008. Nitrofurantoin-induced pulmonary fibrosis: a case report. *J. Med. Case Rep.* 2, 169. <https://doi.org/10.1186/1752-1947-2-169>.
- Hall, B.S., Bot, C., Wilkinson, S.R., 2011. Nifurtimox activation by trypanosomal type I nitroreductases generates cytotoxic nitrile metabolites. *J. Biol. Chem.* 286, 13088–13095. <https://doi.org/10.1074/jbc.M111.230847>.
- Largeron, M., Fleury, M.-B., 1991. Electrochemical synthesis of 2-substituted 5-aminofurans. *Tetrahedron Lett.* 32, 631–634. [https://doi.org/10.1016/S0040-4039\(00\)74846-5](https://doi.org/10.1016/S0040-4039(00)74846-5).
- Leite, A.C.L., Moreira, D.R. de M., Coelho, L.C.D., de Menezes, F.D., Brondani, D.J., 2008. Synthesis of aryl-hydrazones via ultrasound irradiation in aqueous medium. *Tetrahedron Lett.* 49, 1538–1541. <https://doi.org/10.1016/j.tetlet.2007.12.103>.
- Letelier, M.E., Izquierdo, P., Godoy, L., Lepe, A.M., Faúndez, M., 2004. Liver microsomal biotransformation of nitro-aryl drugs: mechanism for potential oxidative stress induction. *J. Appl. Toxicol.* 24, 519–525. <https://doi.org/10.1002/jat.999>.
- Letelier, M.E., Molina-Berrios, A., Cortés-Troncoso, J., Jara-Sandoval, J.A., Müller, A., Aracena-Parks, P., 2010. Comparative effects of superoxide anion and hydrogen peroxide on microsomal and cytosolic glutathione S-transferase activities of rat liver. *Biol. Trace Elem. Res.* 134, 203–211. <https://doi.org/10.1007/s12011-009-8461-3>.
- Letelier, M.E., Hidalgo-Castro, F., López-Valladares, M., Ibacache, N., Pérez, C., Brunner, J., González, J., Gutmann, R., Lazo-Henríquez, C., Gallardo-Garrido, C., Molina-Berrios, A., Ossandón, E., 2017. BG126<sup>®</sup> phytodrug improves urinary tract infection treatment with nitrofurantoin in adult women in a double-blind randomized clinical trial. *J. Herb. Med.* 9, 60–67. <https://doi.org/10.1016/j.hermed.2017.03.001>.
- Li, H., Zhang, Z., Yang, X., Mao, X., Wang, Y., Wang, J., Peng, Y., Zheng, J., 2019. Electron deficiency of nitro group determines hepatic cytotoxicity of Nitrofurantoin. *Chem. Res. Toxicol.* 32, 681–690. <https://doi.org/10.1021/acs.chemrestox.8b00362>.
- Lowry, O.H., Rosebrough, N.J., Farr, A.L., Randall, R.J., 1951. Protein measurement with the Folin phenol reagent. *J. Biol. Chem.* 193, 265–275.
- Morales, A., Richter, P., Inés Toral, M., 1987. Voltammetric behaviour of nitrofurazone, furazolidone and other nitro derivatives of biological importance. *Analyst* 112, 965–970. <https://doi.org/10.1039/an9871200965>.
- Moreno, S.N., Mason, R.P., Docampo, R., 1984. Reduction of nifurtimox and nitrofurantoin to free radical metabolites by rat liver mitochondria. Evidence of an outer membrane-located nitroreductase. *J. Biol. Chem.* 259, 6298–6305.
- Núñez-Vergara, L.J., Sturm, J.C., Olea-Azar, C., Navarrete-Encina, P., Bollo, S., Squella, J.A., 2000. Electrochemical, UV-visible and EPR studies on nitrofurantoin: nitro radical anion generation and its interaction with glutathione. *Free Radic. Res.* 32, 399–409. <https://doi.org/10.1080/10715760000300401>.
- Olive, P.L., 1979. Inhibition of DNA synthesis by nitroheterocycles I. correlation with half-wave reduction potential. *Br. J. Cancer* 40, 89–93. <https://doi.org/10.1038/bjc.1979.144>.
- Perito, B., Allocati, N., Casalone, E., Masulli, M., Dragani, B., Polsinelli, M., Aceto, A., Ilio, C.D.I., 1996. Molecular cloning and overexpression of a glutathione transferase gene from *Proteus mirabilis*. *Biochem. J.* 318, 157–162.
- Pessoa-Mahana, H., Martínez Aránguiz, K.G., Araya-Maturana, R., Pessoa-Mahana, C.D., 2005. A facile approach for new Dibenzo [ b,f ][1,5] Diazocinones. *Synth. Commun.* 35, 1493–1500. <https://doi.org/10.1081/SCC-200057990>.
- Repetto, G., del Peso, A., Zurita, J.L., 2008. Neutral red uptake assay for the estimation of cell viability/ cytotoxicity. *Nat. Protoc.* 3, 1125–1131. <https://doi.org/10.1038/nprot.2008.75>.
- Sandegren, L., Lindqvist, A., Kahlmeter, G., Andersson, D.I., 2008. Nitrofurantoin resistance mechanism and fitness cost in *Escherichia coli*. *J. Antimicrob. Chemother.* 62, 495–503. <https://doi.org/10.1093/jac/dkn222>.
- Sarvi, S., Crispin, R., Lu, Y., Zeng, L., Hurley, T.D., Houston, D.R., von Kriegsheim, A., Chen, C.H., Mochly-Rosen, D., Ranzani, M., Mathers, M.E., Xu, X., Xu, W., Adams, D.J., Carragher, N.O., Fujita, M., Schuchter, L., Unciti-Broceta, A., Brunton, V.G., Patton, E.E., 2018. ALDH1 bio-activates Nifuroxazide to eradicate ALDH high melanoma-initiating cells. *Cell Chem. Biol.* 25, 1456–1469.e6. <https://doi.org/10.1016/j.chembiol.2018.09.005>.
- Schwan, T.J., Ebetino, F.H., 2000. Antibacterial Agents, Nitrofurans, in: Kirk-Othmer Encyclopedia of Chemical Technology. John Wiley & Sons, Inc, Hoboken, NJ, USA, pp. 1043–1081. <https://doi.org/10.1002/0471238961.1409201819030823.a01>.
- Wang, Y., Gray, J.P., Mishin, V., Heck, D.E., Laskin, D.L., Laskin, J.D., 2008. Role of cytochrome P450 reductase in nitrofurantoin-induced redox cycling and cytotoxicity. *Free Radic. Biol. Med.* 44, 1169–1179. <https://doi.org/10.1016/j.freeradbiomed.2007.12.013>.
- Wolfe, K.L., Rui, H.L., 2007. Cellular antioxidant activity (CAA) assay for assessing antioxidants, foods, and dietary supplements. *J. Agric. Food Chem.* 55, 8896–8907. <https://doi.org/10.1021/jf0715166>.
- Yang, F., Hu, M., Lei, Q., Xia, Y., Zhu, Y., Song, X., Li, Y., Jie, H., Liu, C., Xiong, Y., Zuo, Z., Zeng, A., Yu, L., Shen, G., Wang, D., Xie, Y., Ye, T., Wei, Y., 2015. Nifuroxazide induces apoptosis and impairs pulmonary metastasis in breast cancer model. *Cell Death Dis.* 6, e1701. <https://doi.org/10.1038/cddis.2015.63>.
- Zhou, L., Ishizaki, H., Spitzer, M., Taylor, K.L., Temperley, N.D., Johnson, S.L., Brear, P., Gautier, P., Zeng, Z., Mitchell, A., Narayan, V., McNeil, E.M., Melton, D.W., Smith, T.K., Tyers, M., Westwood, N.J., Patton, E.E., 2012. ALDH2 mediates 5-nitrofurantoin activity in multiple species. *Chem. Biol.* 19, 883–892. <https://doi.org/10.1016/j.chembiol.2012.05.017>.